Journal of
Translational Regenerative Medicine

2026. Volume 1

Research Paper

# Development of a Cellulose Based Hydrogel Scaffold Incorporated With Gelatin and βTricalcium Phosphate for Wound Healing

**Nader Nezafati[1*], Maryam Tahmasebi[1], Saeed Hesaraki[1], Elham Taghizadeh[2], Sara Keshtkari[3]**

*1. Biomaterials Group, Department of Nanotechnology and Advanced Materials, Materials and Energy Research Center, Karaj, Iran.*
*2. Department of Medical Science, Bam University of Medical Science, Bam, Iran.*
*3. Department of Internal Medicine, Aja University of Medical Sciences, Tehran, Iran*

Use your device to scan and read the article online

**Citation** Nezafati N, Tahmasebi M, Hesaraki S, Taghizadeh E, Keshtkari S. Development of a Cellulose Based Hydrogel Scaffold Incorporated With Gelatin and βTricalcium Phosphate for Wound Healing. Journal of Translational Regenerative Medicine. 2025; 1:E1017. http://dx.doi.org/10.32598/JTRM.1.1017

http://dx.doi.org/10.32598/JTRM.1.1017

## ABSTRACT

**Background:** The development of a scaffold capable of providing a suitable environment for bone regeneration faces significant challenges. In addition to meeting the requirements related to material selection and fabrication techniques, a bone scaffold must ensure adequate porosity to facilitate osteogenesis and vascularization, while also maintaining sufficient mechanical strength during the early stages of bone healing and recovery.

**Methods:** A biodegradable cellulose-based hydrogel scaffold composed of hydroxyethyl cellulose (HEC), hydroxypropyl methylcellulose (HPMC), gelatin, and β-tricalcium phosphate (β-TCP) was developed for wound-healing applications using a freeze-drying technique. Different formulations of HEC/HPMC/gelatin/β-TCP scaffolds were initially prepared. To evaluate scaffold performance, Fourier transform infrared spectroscopy (FTIR), scanning electron microscopy (SEM), mechanical testing, degradation analysis, swelling measurements, and antibacterial assays were performed.

**Results:** Among the prepared formulations, the HEC70–HPMC30 scaffold showed the most favorable mechanical properties, with a tensile strength of approximately 30 MPa, Young's modulus of 1800 MPa, and elongation at break of ~2%. The scaffold also displayed a highly porous interconnected structure with an average pore size of nearly 100 μm. To improve structural stability, gelatin crosslinked with genipin was incorporated into the optimized polymer matrix, extending the degradation time from approximately 1 h to 24 h. Subsequently, β-TCP was added at concentrations of 10, 20, and 30 wt/v%. SEM observations revealed that increasing β-TCP content promoted a more organized pore architecture and more uniform pore distribution. FTIR and elemental mapping analyses confirmed the successful incorporation and homogeneous distribution of β-TCP within the scaffold network. The incorporation of β-TCP significantly affected the physicochemical properties of the scaffolds. Water uptake decreased from 712% in the control scaffold to 402% in the scaffold containing the highest β-TCP concentration after 9 h, while degradation after 24 h decreased to approximately 85%, indicating enhanced structural stability. However, no antibacterial activity was observed against *Escherichia coli* or *Staphylococcus aureus*.

**Article info:**
**Received:** 25 Jun 2026
**Accepted:** 23 Jul 2026
**Publish:** 12 Aug 2026

*** Corresponding Author:**
*Nader Nezafati, Associate Professor.*
***Address:*** *Biomaterials Group, Department of Nanotechnology and Advanced Materials, Materials and Energy Research Center, Karaj, Iran.*
***Phone:*** *+98 (26) 36280040*
***E-mail:*** *n.nezafati@merc.ac.ir*

Copyright © 2026 The Author(s);
This is an open access article distributed under the terms of the Creative Commons Attribution License (CC-By-NC: https://creativecommons.org/licenses/by-nc/4.0/legalcode.en), which permits use, distribution, and reproduction in any medium, provided the original work is properly cited and is not used for commercial purposes.

**Conclusion:** The developed HEC/HPMC/gelatin/β-TCP scaffolds exhibit favorable mechanical performance, controlled degradation, and improved structural stability, demonstrating their potential as promising candidates for wound healing.

**Keywords:** Hydroxyethyl cellulose (HEC), Hydroxypropyl methylcellulose (HPMC), Scaffold, Mechanical test, Biodegradation, Antibacterial assay

## Highlights

- A biodegradable cellulose-based hydrogel scaffold composed of HEC/HPMC, gelatin, and β-TCP was successfully developed for wound healing.
- The HEC70/HPMC30 scaffold exhibited high porosity, with an average pore size of approximately 100 μm, and tensile strength close to 30 MPa.
- Incorporation of genipin-crosslinked gelatin and β-TCP significantly improved structural stability, pore organization, and degradation behavior of the scaffolds.
- Increasing β-TCP content reduced water uptake and degradation rate, while no antibacterial activity was observed against *S. aureus* and *E. coli*.

## Plain Language Summary

The cellulose derivatives such as hydroxyethyl cellulose (HEC) and hydroxypropyl methylcellulose (HPMC), have attracted considerable attention for biomedical and tissue engineering applications. In recent decades, ion-mediated bioactive ceramics such as β-tricalcium phosphate (β-TCP) have been extensively investigated for wound-healing applications. In the present study, a cellulose-based hydrogel scaffold composed of HPMC, HEC, gelatin, and β-TCP was fabricated using a freeze-drying technique, followed by genipin-mediated crosslinking. The main goal was to investigate the effects of incorporating β-TCP in the fabricated scaffolds. The results showed that incorporation of genipin-crosslinked gelatin and β-TCP significantly improved structural stability, pore organization, and degradation behavior of the scaffolds. The developed HEC/HPMC/gelatin/β-TCP scaffolds with favorable mechanical performance, controlled degradation, and improved structural stability, have the potential for wound healing.

## Introduction

With the rapid advancement of tissue engineering, which is fundamentally based on the integration of scaffolds, stem cells, and growth factors, a new generation of wound dressings with the potential to accelerate the wound healing process has emerged [1]. Skin tissue engineering employs hydrogel-based constructs composed of natural and synthetic biomaterials to promote scar-free regeneration in critical skin defects and ultimately improve patients' quality of life. Polymeric wound dressings have been extensively investigated because of their ability to provide a moist healing environment, stimulate growth factor release, enhance angiogenesis, and protect the wound site against microbial contamination [2, 3]. Biomaterials are natural or synthetic substances designed to function either independently or as components of more complex systems for therapeutic and diagnostic applications in tissue engineering. In the design of biomaterial-based scaffolds, several critical parameters should be considered to support proper tissue regeneration while minimizing undesirable post-implantation responses. Surface chemistry, mechanical performance, porosity, and protein adsorption capacity are among the most important factors influencing scaffold functionality. In addition, tissue response may be strongly influenced by scaffold architecture, pore-size distribution, and implantation methodology [4]. Table 1 summarizes several commercially available skin substitute products for clinical applications.

**Table 1.** Commercially available skin substitute products for wound healing

| Product Name | Classification | Biomaterial Used | Cells | Indication | Outcomes | Ref. |
|---|---|---|---|---|---|---|
| AlloDerm® | Decellularized | Decellularized human cadaver skin | - | Various | Used in combination with epidermal autografts; positive effect on scar quality; no significant immune response | [5] |
| Apligraf® | Temporary composite allogeneic | Bovine collagen matrix | Fibroblasts and keratinocytes | Chronic wounds | Improved wound closure; no significant immune response; conversion of non-healing wounds to healing wounds | [6] |
| Biobrane® | Decellularized | Silicone membrane bonded to a nylon mesh containing porcine collagen | - | Burns | Reduced infection; accelerated wound closure; pain reduction; adhesion issues; may adhere to tissue over time and require removal | [7] |
| | Temporary or permanent allogeneic | Polyglactin mesh scaffold | Fibroblasts | Chronic wounds | Improved wound closure; no adverse reactions or rejection; increased blood flow | [8] |
| Integra® | Decellularized | Bovine collagen and shark chondroitin sulfate with a silicone membrane | - | Various | Enhanced wound bed vascularization; improved wound closure; fewer side effects; may require a two-stage procedure followed by epidermal autografting | [9] |
| Matriderm® | Decellularized | Bovine collagen and elastin membrane | - | Full-thickness wounds, burns | Used with epidermal autografts; improved wound closure; increased skin elasticity | [10] |
| TransCyte™ | Temporary allogeneic | Silicone membrane bonded to a nylon mesh containing porcine collagen | Fibroblasts | Burns | Reduced healing time; shorter hospital stay; reduced hypertrophic scar formation; excellent handling properties | [10] |

Among naturally derived polymers, cellulose has attracted considerable attention due to its renewability, biocompatibility, biodegradability, abundance, and cost-effectiveness [11, 12]. The abundance of hydrophilic functional groups, including hydroxyl, carboxyl, and aldehyde moieties, within the structure of cellulose and its derivatives makes these materials highly promising candidates for biomedical and tissue engineering applications [13]. Hydroxypropyl methylcellulose (HPMC), a nonionic cellulose derivative composed of linear glucose units, possesses a matrix structure stabilized by hydrogen-bonding interactions [14]. HPMC has emerged as an attractive biomaterial for scaffold fabrication due to its excellent biocompatibility, film-forming capability, favorable rheological properties, and chemical stability [15, 16]. The hydrophilic or hydrophobic behavior of HPMC is closely related to its degree of substitution (DS) and molar substitution (MS). Lower DS and MS values generally result in greater hydrophilicity, whereas higher values increase hydrophobic behavior. Owing to the coexistence of polar hydroxypropyl groups and nonpolar methyl groups, HPMC can establish intermolecular and intramolecular interactions with a wide range of materials. Hydroxyethyl cellulose (HEC) is another nonionic, water-soluble cellulose derivative synthesized through the reaction of cellulose with ethylene oxide. Its structure, enriched with hydroxyl groups, facilitates chemical functionalization and provides advantageous physicochemical characteristics. HEC is widely used in wound dressings, tissue engineering scaffolds, cosmet-

ics, food thickeners, protective colloids, and stabilizing or coating agents. These broad applications are attributed to its high biocompatibility, low toxicity, non-immunogenicity, hydrophilicity, and strong hydrogen-bonding capability associated with its β-D-glucose rings. Such characteristics contribute to its aqueous solubility, enhanced viscosity, thermal plasticity, and colloidal stabilization. Furthermore, the accessible hydroxyl groups in HEC enable the incorporation of various functional moieties, thereby expanding its potential biomedical applications [3, 17, 18]. Figure 1 illustrates the chemical structures of HPMC and HEC [19].

Bioactive ceramics, commonly referred to as bioceramics, have emerged as an important class of biomaterials in regenerative medicine because of their intrinsic bioactivity and tunable physicochemical properties. Ionic products released during the dissolution of bioceramic materials, including calcium (Ca), silicon (Si), magnesium (Mg), and copper (Cu) ions, can provide biochemical signals that can regulate cellular behavior through intracellular signaling pathways. In recent decades, ion-mediated bioactive ceramics have been extensively investigated for wound-healing applications due to their antibacterial activity, angiogenic potential, immunomodulatory effects, promotion of skin appendage regeneration, antitumor properties, and ability to improve mechanical performance [20, 21]. Among these materials, β-tricalcium phosphate (β-TCP) has been widely studied for biomedical and tissue-engineering applications, particularly in bone regeneration and wound repair. Owing to its excellent biocompatibility and biodegradability, β-TCP can gradually resorb within the physiological environment and be replaced by newly formed tissue. Although β-TCP is primarily recognized for bone tissue engineering, its osteoconductive and bioactive characteristics may also be advantageous in complex wound healing conditions, especially in wounds associated with bone exposure [22]. In fact, β-TCP, due to the presence of calcium in its structure, plays a constructive role in skin physiology and wound healing [23]. In the present study, a cellulose-based hydrogel scaffold composed of HPMC, HEC, gelatin, and β-TCP was fabricated using a freeze-drying technique, followed by genipin-mediated crosslinking. The main goal was to investigate the effects of incorporating β-TCP in the physicochemical, morphological, degradation, swelling, and antibacterial properties of the fabricated scaffolds.

## Materials and Methods

### Materials

The raw materials used for scaffold fabrication included HEC (Number: 822068, Sigma-Aldrich), HPMC (Number: 423238, Sigma-Aldrich), gelatin (Number: 104070, Merck), β-TCP, genipin (Number: 6902-77-8, Merck), citric acid (Number: 77-92-9, Merck), sodium chloride (Number: 7647-14-5, Samchun), potassium chloride (Number: 7447-40-7, Samchun), disodium phosphate (Number: 7758-79-4, Samchun), and monopotassium phosphate (Number: 7778-77-0, Samchun).

### Scaffold preparation

To fabricate scaffolds composed of HEC and HPMC, a 3 wt% HEC solution was first prepared and stirred on a magnetic stirrer at 70 ˚C for 1 h. Subsequently, a 2 wt% HPMC solution was prepared and stirred at room temperature for 30 min. The HEC and HPMC solutions were then mixed at different volume-to-volume ratios and further stirred on a magnetic stirrer for an additional 1 h. To prepare gelatin- and genipin-containing scaffolds, the HEC/HPMC solution was first synthesized according to the aforementioned procedure. Subsequently, gelatin solutions containing 10, 20, and 30 wt% gelatin were added to the hydrogel at a concentration corresponding to 20 wt% of the base polymers. For this purpose, gelatin was first dissolved in deionized water at 50 ˚C, after which 140 µL of a 0.3 wt% genipin solution was added. The resulting solution was then incorporated into the HEC/HPMC mixture at room temperature. The prepared solutions were poured into 35-mm-diameter Petri dishes and maintained at room temperature for 48 h to

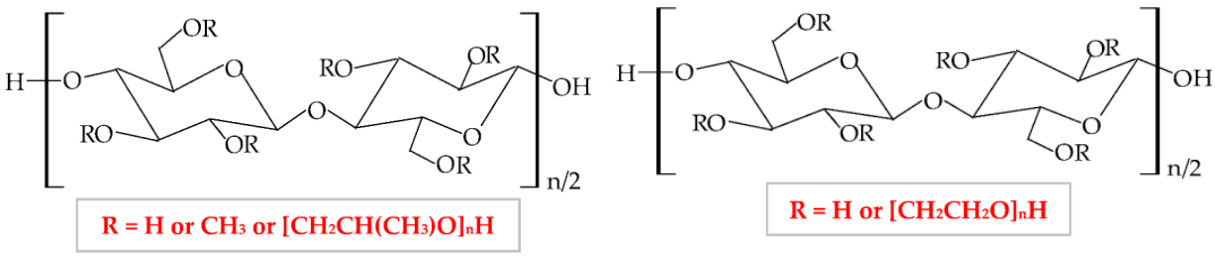


**Figure 1.** Chemical structures of HPMC and HEC [19]

allow film formation. In addition, to compare the degradation behavior of the scaffolds, a scaffold containing 30 wt% gelatin with a 50:50 gelatin-to-genipin ratio was fabricated and evaluated. Following the evaluation of scaffold degradation time, the formulation containing 30 wt% gelatin at 20 wt% relative to the base polymers was selected as the optimal composition.

To prepare the final scaffold, we mixed HEC, HPMC, gelatin, β-TCP, and genipin (as a crosslinking agent). The HEC/HPMC/gelatin/genipin solution was first prepared as previously described, and β-TCP at different concentrations was subsequently added to the mixture. All samples were cast into cylindrical molds with a diameter of 10 mm, frozen at −80 ˚C for 24 h, and subsequently freeze-dried under vacuum at −57 ˚C for 48 h using a lyophilizer. Table 2 presents the designation codes of the scaffolds containing gelatin and β-TCP, along with their corresponding weight percentages.

## Scaffold characterization

### Scanning electron microscopy (SEM)

The morphology of the fabricated scaffolds was evaluated using SEM. Prior to imaging, the samples were sputter-coated with gold for 10 min and subsequently examined using a scanning electron microscope. In addition, scaffold porosity was measured using ImageJ software, version 1.54p).

### Fourier transform infrared spectroscopy (FTIR)

FTIR was employed to investigate the functional groups present in the scaffolds. The spectra were recorded within the range of 400–4000 $cm^{-1}$ with a spectral resolution of 1 $cm^{-1}$.

### Tensile strength testing

To evaluate the mechanical properties of the scaffolds, a uniaxial tensile strength test was performed in accordance with ASTM D882 (ASTM, 2001). For this purpose, scaffold specimens with approximate dimensions of 50×20 mm were prepared, and their stress–strain curves were recorded using a tensile testing machine with a 10 N load cell and a crosshead speed of 50 mm/min. Following the acquisition of the stress–strain curves, tensile strength, Young's modulus, and elongation at break were determined. The Mean±SD of three samples were reported.

## Degradation analysis

### Preparation of PBS solution

Phosphate-buffered saline (PBS) solution was used to evaluate scaffold swelling and degradation behavior. To prepare the PBS solution, the salts were sequentially dissolved in 800 mL of deionized water, and the final volume was adjusted to 1000 mL by adding deionized water [24].

### Immersion procedure

To evaluate the degradation behavior of the synthesized scaffolds, each scaffold with a specified initial weight ($W_0$) was immersed in PBS at pH 7.4 and room temperature. The samples were then incubated at 37 ˚C for 0.5, 2, 4, 6, and 24 h. At the end of each immersion period, the scaffolds were completely dried and weighed to determine the final weight after degradation (Wt). Finally, the degradation percentage of each sample was calculated as follows (Equation 1):

1. $Degradation\ (\%)=((W_0-Wt)/W_0)\times 100$

## Water uptake analysis

To determine the water absorption capacity of the scaffolds, a specified weight of each sample ($W_1$) was immersed in 10 mL of PBS solution at 37 ˚C. During a 9-h period, the samples were removed from the solution at predetermined intervals, and excess surface water was gently removed using filter paper. The wet weight after immersion ($W_2$) was then measured. The water uptake percentage was calculated using the Equation 2:

2. $Water\ uptake\ (\%)=((W_2-W_1)/W_1)\times 100$

## Antibacterial assay

The antibacterial activity of β-TCP against the gram-negative bacterium *Escherichia coli* and the gram-positive bacterium *Staphylococcus aureus* was evaluated using the disk diffusion method. Fresh bacterial cultures were used to prepare suspensions equivalent to a 0.5 McFarland standard ($1.5\times10^8$ CFU/mL). The bacterial suspensions were uniformly spread onto solid culture media. Subsequently, test samples at concentrations of 10, 15, 20, 30, and 35 mg/mL were prepared in sterile distilled water, and 100 µL of each concentration was loaded onto sterile paper disks. After complete absorption of the samples onto the disks, the disks were placed on the agar plates. The plates were incubated at 37 ˚C for 48 h. Antibacterial activity was then assessed based on the formation of inhibition zones around the disks [25].

**Table 2.** The codes of gelatin- and β-TCP-containing scaffolds and their corresponding weight percentages

| Sample Code | β-TCP (w/v%) | Gelatin (v/v%) |
|---|---|---|
| C | 0 | 20 |
| S1 | 10 | 20 |
| S2 | 20 | 20 |
| S3 | 30 | 20 |

## Results

Initially, the influence of genipin concentration on scaffold degradation behavior was evaluated. A scaffold containing 30 wt% gelatin with a gelatin-to-genipin ratio of 50:50 was compared with a scaffold containing 30 wt% gelatin crosslinked with three drops of a 0.3 wt% genipin solution over a 1-h incubation period. As illustrated in Figure 2, no considerable difference in scaffold disintegration time was observed between the two formulations, indicating that increasing the genipin concentration beyond the selected level did not further enhance scaffold stability.

### Morphological characterization

As shown in Figure 3, the incorporation of increasing amounts of β-tricalcium phosphate progressively modified the scaffold microstructure, leading to improved pore organization, enhanced structural alignment, and greater pore uniformity in samples S1–S3 compared with the control scaffold.

As shown in Figures 4 and 5, elemental analysis and elemental mapping confirmed the successful incorporation and homogeneous distribution of β-tricalcium phosphate within the scaffold structure. The detected elements included calcium, phosphorus, oxygen, carbon, and nitrogen, with nitrogen originating from the amine groups of gelatin. Furthermore, increasing the β-TCP content from S1 to S3 led to a more extensive distribution and higher concentrations of calcium and phosphorus throughout the scaffold matrix, confirming the progressive incorporation of the ceramic phase.

### FTIR analysis

In the control spectrum, characteristic peaks corresponding to O–H stretching at 3440 $cm^{-1}$, C–H stretching at 2940 $cm^{-1}$, gelatin amide I and II bands at 1656 $cm^{-1}$ and 1554 $cm^{-1}$, CH2 bending at 1453 $cm^{-1}$, and C–O–

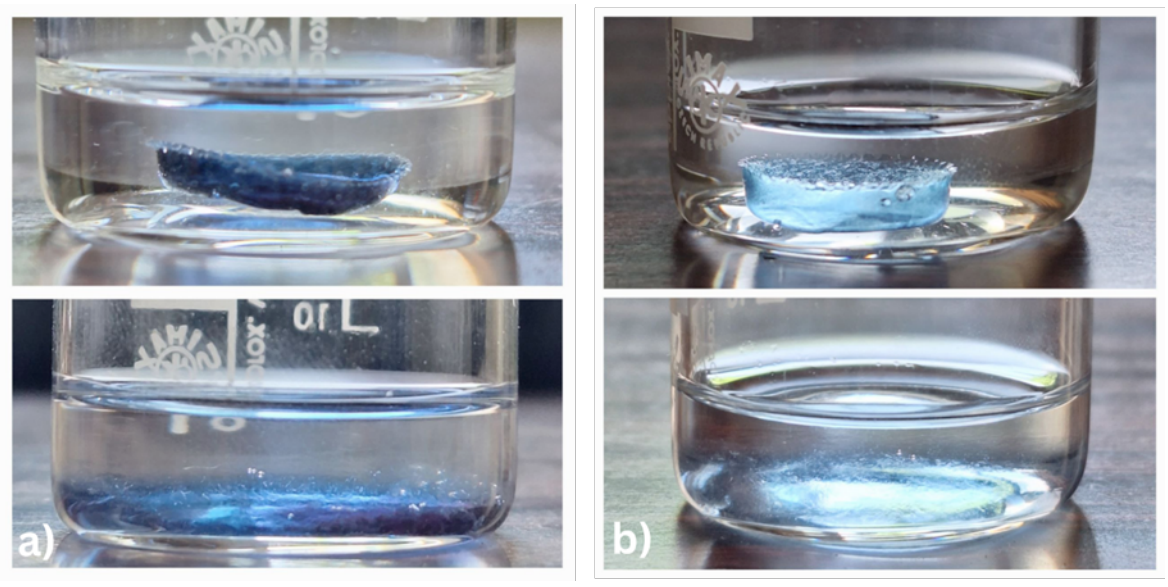


**Figure 2.** Network disintegration after 1 h

a) scaffold containing gelatin and genipin at a 50:50 ratio, b) Scaffold containing gelatin and three drops of genipin

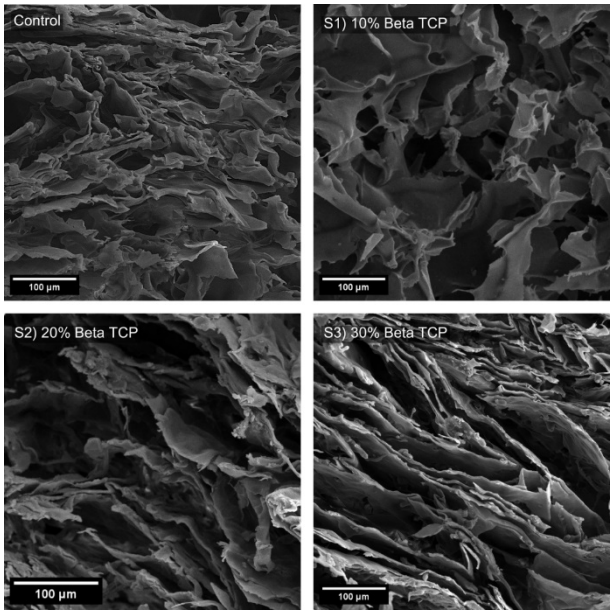


**Figure 3.** SEM images of the scaffolds: Control sample, (S1) the sample containing 10% β-TCP, (S2) the sample containing 20% β-TCP, and (S3) the sample containing 30% β-TCP

C stretching of polysaccharides at 1062 $cm^{-1}$ were observed [3, 26, 27]. After the incorporation of β-TCP into the scaffold matrix, the intensity of the peak at 1062 $cm^{-1}$ increased, indicating overlap with the $PO_4^{3-}$ stretching vibration of β-TCP. In addition, new peaks appeared at 947 $cm^{-1}$ ($PO_4^{3-}$ stretching mode) and 562–596 $cm^{-1}$ (O–P–O bending mode), which are characteristic of β-TCP [27]. These spectral changes became more pronounced as the β-TCP content increased from 10% to 30%. Moreover, the primary polymeric structure was retained after the incorporation of β-TCP. However, slight shifts in the position of some peaks, such as the shift from 1062 $cm^{-1}$ to 1068 $cm^{-1}$ in the scaffold containing 30% β-tricalcium phosphate, suggest interactions between the polymeric matrix and β-TCP particles. These observations confirm the successful incorporation of β-TCP into the polymeric network, as illustrated in Figure 6.

## Mechanical test

The tensile strength test results of the scaffolds indicate that the combination of HPMC and HEC has a significant effect on the mechanical properties of the scaffolds (Figure 7). The HEC70–HPMC30 sample exhibited the best overall performance, showing the highest tensile strength, Young's modulus, and elongation at break. This composition enhanced the mechanical strength compared with pure HEC. Pure HEC demonstrated the lowest tensile strength and Young's modulus (Table 3); however, it exhibited the greatest flexibility, with an elongation at break of approximately 2.06%. In general, increasing the HPMC content reduced scaffold flexibility, as evidenced by the HEC30–HPMC70 sample, which showed the lowest elongation at break.

All samples displayed similar stress–strain behavior, characterized by an initial linear elastic region followed by a nonlinear region until fracture. The HEC50–HPMC50 and HEC30–HPMC70 samples exhibited intermediate mechanical properties between those of pure HEC and the HEC70–HPMC30 scaffold. HPMC has also been reported to exert a similar influence on the mechanical properties of starch-based scaffolds. In a previous study, the scaffold containing the highest proportion of hydroxypropyl methylcellulose exhibited the greatest tensile strength after five weeks of storage [28]. Furthermore, the tensile strengths of scaffolds composed of different ratios of ethyl cellulose (EC) and hydroxypropyl methylcellulose (HPMC) in the dry state were reported as 4.81, 4.90, and 6.45 MPa for EC/HPMC ratios of 95:5, 90:10, and 85:15, respectively. These findings confirmed that the incorporation of HPMC improved the tensile strength of EC-based scaffolds [29].

## Water uptake behavior

The incorporation of HPMC contributed to the formation of larger pores within the scaffold structure, thereby facilitating greater water uptake and retention. With the incorporation of β tricalcium phosphate and increasing its concentration, the swelling ratio decreased. This reduction can be attributed to the non-hydrophilic na-

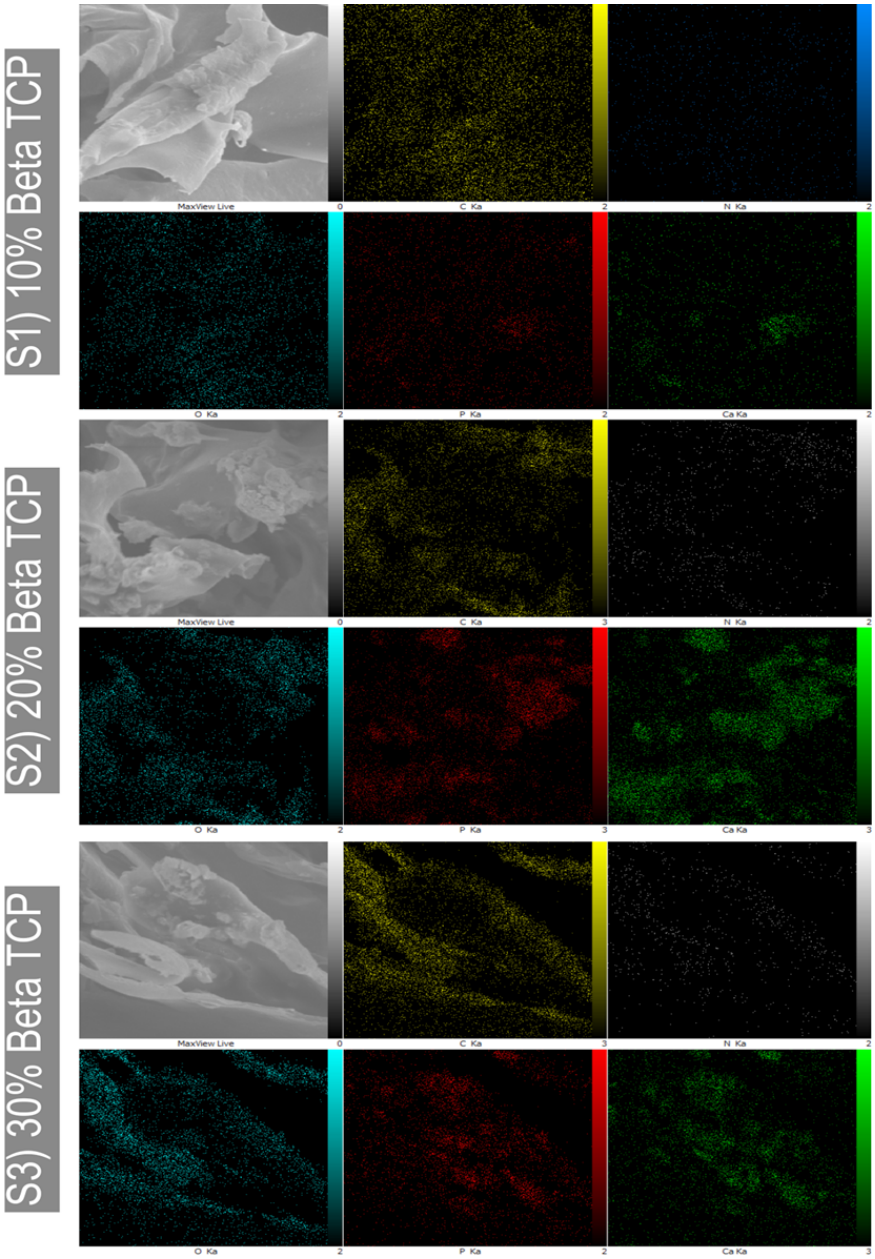


**Figure 4.** Elemental mapping of the scaffolds. )S1) containing 10% β-TCP, (S2) containing 20% β-TCP, and (S3) containing 30% β-TCP

ture of β tricalcium phosphate, which lowers the overall water absorption capacity of the scaffold [30]. The swelling rate was fastest during the first 2 hours for all compositions and gradually slowed thereafter. This pattern indicates rapid initial water uptake, followed by a reduction in the absorption rate as the scaffold gradually approached saturation (Figure 8).

## Biodegradation behavior

The degradation test was conducted over a period of 24 hours. The results indicate that all compositions exhibited an increase in degradation percentage over time, although with a pattern different from that observed in the swelling behavior. The base composition showed the highest degradation rate, reaching approximately 85% degradation after 24 hours. This finding indicates the relatively low stability of this composition in an aqueous environment. With increasing β tricalcium phosphate content, the degradation rate decreased significantly, indicating that β tricalcium phosphate acts as a stabilizing agent and enhances the resistance of the scaffold against degradation. In contrast to the swelling pattern, the degradation rate was relatively slow during the first 6 hours; however, a significant increase in degradation was observed between 6 and 24 hours. This

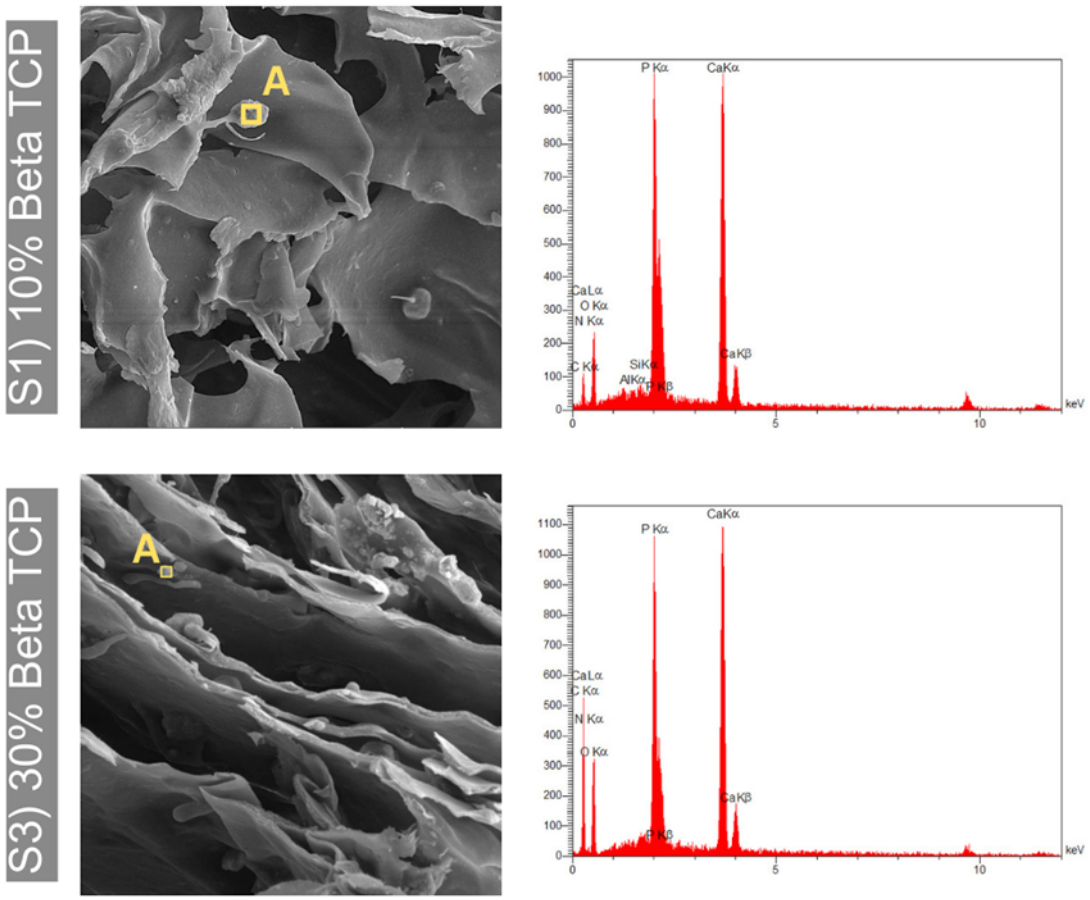


**Figure 5.** Elemental analysis of the scaffolds. (S1) containing 10% β-TCP, (S3) containing 30% β-TCP

pattern may indicate the presence of a delay phase at the beginning of the degradation process, after which degradation proceeds more rapidly. As shown in Figure 9, the incorporation of β-tricalcium phosphate reduced the degradation rate of the scaffolds, and increasing the β-tricalcium phosphate content led to greater scaffold stability in the aqueous environment.

### Antibacterial activity

### Inhibition zone assay

To evaluate the antibacterial activity of the scaffolds, a Gram positive bacterium (*S. aureus*) and a Gram negative bacterium (*E. coli*) were used. Based on the obtained results, no inhibition zones were observed in the plates containing the scaffolds. These findings are consistent with previous studies investigating the antibacterial properties of scaffolds containing hydroxyethyl cellulose [3], hydroxypropyl methylcellulose [26], and β tricalcium phosphate [31]. Studies have shown that the addition of 45S5 bioglass to β TCP scaffolds can induce antimicrobial behavior that is not present in pure β TCP, thereby preventing the adhesion and proliferation of microorganisms. This behavior can be attributed to the release of ionic species from bioglass into the surrounding medium and the subsequent increase in local pH. The change in pH may alter osmotic pressure, disrupt the integrity of the cytoplasmic membrane, and lead to protein denaturation, which ultimately affects intracellular functions such as enzyme activity that are essential for the cellular metabolism of microorganisms. As shown in Figures 10 and 11, neither the control scaffold nor the β-tricalcium phosphate-containing scaffolds exhibited detectable inhibition zones against E. coli or S. aureus, confirming the absence of significant antibacterial activity regardless of β-TCP concentration.

## Discussion

β-TCP plays a significant role in the freeze-drying process and ice crystal formation, ultimately exerting a considerable effect on scaffold morphology. This mineral phase influences the final scaffold architecture through several mechanisms occurring during the freezing and

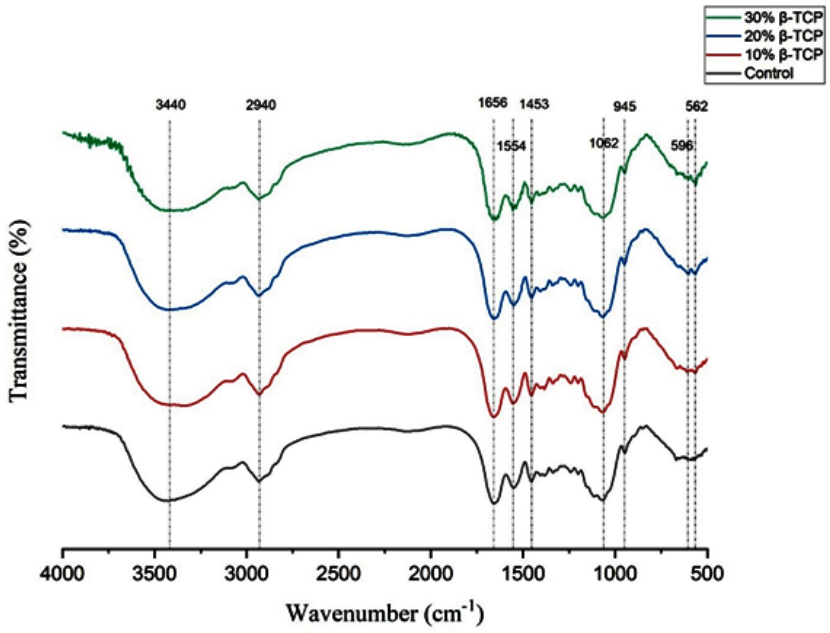


**Figure 6.** FTIR spectra of the control sample and the scaffolds containing 10%, 20%, and 30% β-TCP

drying processes. During the freezing stage, β-TCP particles act as nucleation sites for ice crystal formation. This phenomenon can lead to the generation of smaller and more uniformly distributed ice crystals, ultimately resulting in a more homogeneous porous scaffold structure [32]. Furthermore, the presence of β-TCP particles can alter the growth pattern of ice crystals, leading to the formation of ice structures with different morphologies. Following sublimation, these altered structures produce pores with diverse shapes and sizes in the final scaffold [33]. The incorporation of β-TCP into the polymeric solution can also modify its viscosity and thermal properties. These changes influence the freezing rate and consequently affect the size and morphology of the formed ice crystals [34, 35]. In addition, β-TCP particles may introduce structural heterogeneity, which can result in the formation of pores with varying sizes and shapes within the final scaffold [36]. The presence of β-TCP can further affect the sublimation process, thereby influencing the final pore morphology and dimensions of the scaffold [37]. These morphological modifications may substantially affect scaffold performance in tissue engineering applications. For instance, alterations in pore size and distribution can influence cell infiltration, adhesion, and proliferation. Likewise, changes in porosity and pore interconnectivity may affect nutrient and oxygen transport throughout the scaffold structure [38]. The SEM images obtained from the freeze-dried scaffolds demonstrated considerable structural and morphological changes with increasing β-TCP concentration. At lower concentrations, the pores appeared more irregular, whereas increasing β-TCP content resulted in a more organized pore architecture with more uniform dimensions [39]. In the control sample, the scaffold structure consisted of thin and wrinkled sheets forming a complex porous network. This structure appeared relatively homogeneous throughout the sample. Upon incorporation of β-tricalcium phosphate, gradual yet significant structural modifications were observed. In the scaffold containing 10% β-TCP, the structure became more open, larger pores were visible, and the sheets appeared thicker and mechanically more robust. As the β-TCP concentration increased to 20% and subsequently 30%, this trend became more pronounced. In the 30% β-TCP scaffold, the structure appeared entirely different, exhibiting longer, more parallel, and highly organized sheets. Simultaneously, increasing β-TCP concentration led to a greater presence of fine β-TCP particles throughout the scaffold matrix. These particles were uniformly distributed within the structure and appeared to be well integrated with the polymeric matrix. Such integration may contribute to enhanced mechanical properties and improved bioactivity of the scaffolds [40]. The observed alterations in scaffold structure and porosity with increasing β-TCP concentration may significantly influence their performance in tissue engineering applications. Increased porosity and pore size may improve cell infiltration, adhesion, and proliferation. Moreover, the more organized architecture observed at higher β-TCP concentrations may facilitate guided tissue growth [41].

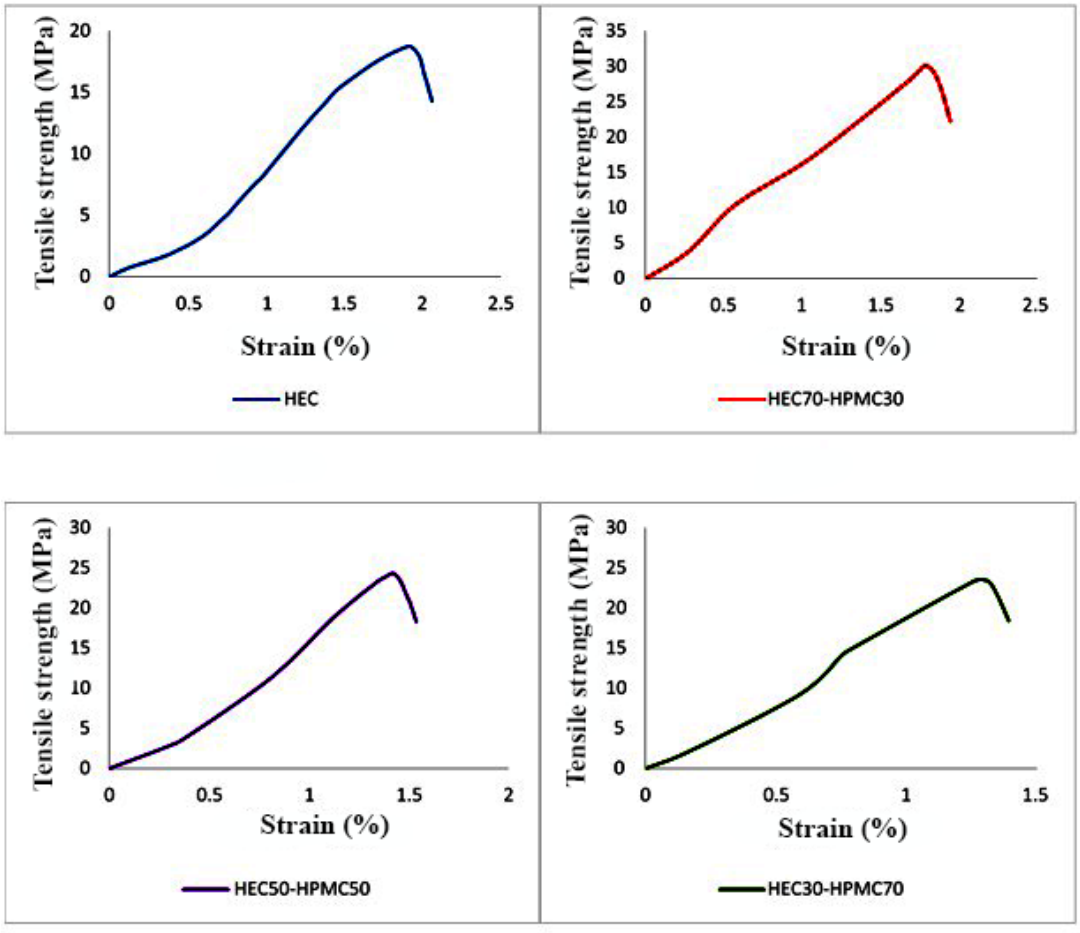


**Figure 7.** The tensile strength test results for the scaffolds

The FTIR spectra were used to analyze the chemical structure of the control sample and the scaffolds containing different concentrations of β-tricalcium phosphate. The control sample consisted of hydroxyethyl cellulose, hydroxypropyl methylcellulose, gelatin, and genipin.

The changes in mechanical values can be attributed to the formation of new molecular interactions between HPMC and HEC, resulting in the development of a stronger polymeric network. Differences in the chemical structure and molecular weight of the two polymers influence the arrangement and packing of the polymer chains. Moreover, the addition of HPMC may alter the overall degree of crystallinity of the system, which is typically associated with increased stiffness and reduced flexibility [29]. In addition, differences in the hydrophilic characteristics of HPMC and HEC can affect moisture absorption and, consequently, the mechanical properties of the scaffolds [19]. Overall, these results

**Table 3.** Mechanical test results for the scaffolds

| Sample | Mean±SD | | Strain (%) |
|---|---|---|---|
| | Tensile Strength (MPa) | Elastic Modulus (MPa) | |
| HEC | 18.73±0.38 | 874.27±1.28 | 2.06±0.8 |
| HEC70-HPMC30 | 30.13±0.47 | 1836.91±1.01 | 1.94±0.11 |
| HEC50-HPMC50 | 24.32±0.65 | 1117.99±1.34 | 1.53±0.9 |
| HEC30-HPMC70 | 23.37±0.55 | 1382.97±0.83 | 1.39±0.7 |

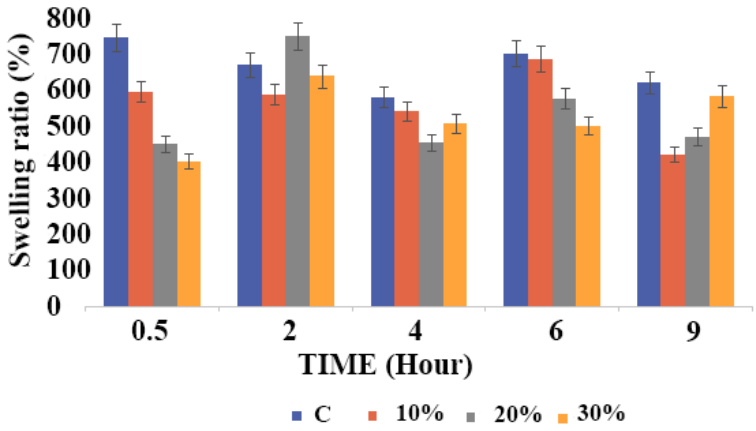


**Figure 8.** Comparing the swelling behavior of the control sample and the scaffolds containing β-TCP

suggest that the incorporation of an optimal amount of HPMC (approximately 30%) into HEC can effectively enhance the mechanical performance of the scaffold by providing a suitable balance between strength and flexibility, making it a promising candidate for wound dressing applications.

The swelling behavior of the freeze-dried scaffolds was evaluated over a period of 9 hours. According to the obtained results, the base composition, which consisted only of hydroxyethyl cellulose, hydroxypropyl methylcellulose, and gelatin, exhibited the highest swelling ratio, reaching approximately 600% at the end of 9 hours. This finding indicates the high-water absorption capacity of these hydrophilic polymers [19]. It is also associated with the formation of hydrogen bonds between hydroxyethyl cellulose and hydroxypropyl methylcellulose, as well as their ability to absorb and retain water [26].

The results of biodegradation demonstrate that the incorporation of β tricalcium phosphate effectively reduces both the swelling and degradation of the scaffolds. This provides the possibility of tailoring scaffold properties for various tissue engineering applications, where precise control over swelling and degradation rates can be critical for optimal scaffold performance. β Tricalcium phosphate influences the scaffold properties in several ways. First, as a ceramic material, it does not absorb water in the same manner as the hydrophilic polymers present in the base composition, thereby reducing the overall swelling behavior. Second, β tricalcium phosphate is more stable in aqueous environments and acts as a physical barrier that protects the polymeric matrix from rapid hydrolysis, consequently reducing the degradation rate. In addition, β tricalcium phosphate particles act as reinforcing agents within the polymer matrix and enhance structural stability. This contributes to both reduced swelling and slower degradation. The addition of β tricalcium phosphate also alters the overall physicochemical properties of the scaffold, which affects how water interacts with the material [30]. β Tricalcium phosphate may also produce a localized buffering effect that

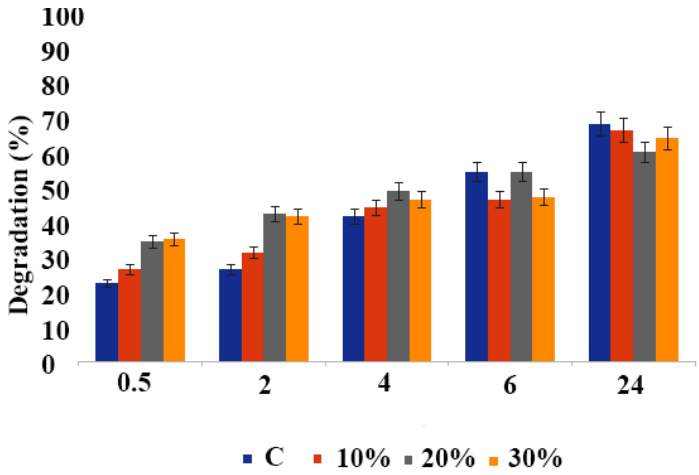


**Figure 9**. Comparing the biodegradability of the control sample and the scaffolds containing β-TCP

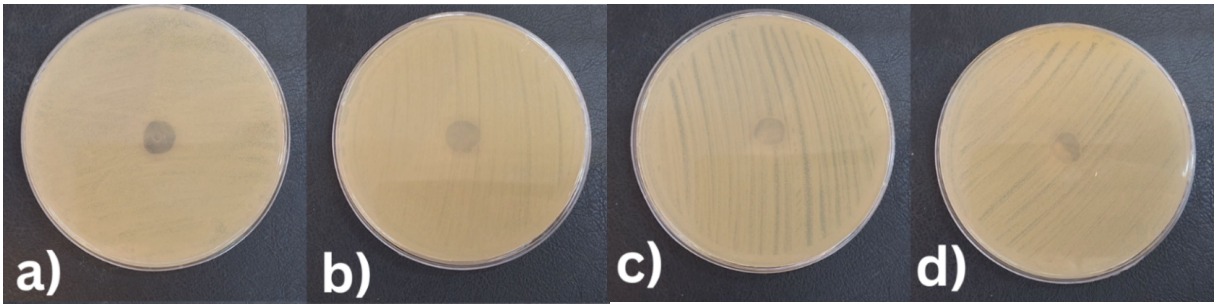


**Figure 10.** Results of inhibition zone assay against *E. coli*

a) Control sample, b) Scaffold containing 10% β-TCP, c) Scaffold containing 20% β-TCP, d) Scaffold containing 30% β-TCP

helps stabilize the pH within the scaffold microenvironment. This effect can influence the degradation rate of the polymeric components. Furthermore, the incorporation of β tricalcium phosphate particles may alter the surface area and surface properties of the scaffold, which can affect the initial water absorption and the accessibility of water to the degradable polymer components [42]. Ultimately, these effects of β tricalcium phosphate contribute to the formation of a more stable scaffold with tunable properties. This enables improved control over swelling and degradation rates for specific biomedical applications. By adjusting the percentage of β tricalcium phosphate, scaffolds with different swelling and degradation characteristics can be designed for various applications in tissue engineering and regenerative medicine.

Concerning antibacterial assessment, although tricalcium phosphate (TCP) does not possess intrinsic antibacterial activity, its incorporation into wound-healing scaffolds remains highly advantageous due to its excellent bioactivity, biocompatibility, and regenerative potential [43]. The beneficial role of TCP in wound repair is primarily associated with its ability to create a favorable microenvironment for tissue regeneration rather than directly inhibiting microbial growth. One of the most important functions of TCP is its gradual degradation and subsequent release of calcium ($Ca^{2+}$) and phosphate ($PO_4^{3-}$) ions. These ions play critical roles in cellular signaling pathways involved in tissue repair, including fibroblast proliferation, cell migration, extracellular matrix deposition, and angiogenesis. Calcium ions, in particular, are known to regulate various stages of the wound-healing cascade and contribute to the formation of granulation tissue and re-epithelialization [44]. Furthermore, the bioactive surface of TCP promotes protein adsorption and cell attachment, thereby facilitating cellular colonization and tissue integration. In addition, TCP exhibits excellent biodegradability and bioresorbability, allowing it to gradually dissolve and be replaced by newly formed tissue. This controlled degradation process not only provides temporary structural support but also continuously supplies bioactive ions that stimulate tissue regeneration. The porous structure commonly associated with TCP-containing scaffolds further enhances nutrient diffusion, oxygen transport, vascular ingrowth, and cellular infiltration, all of which are essential for efficient wound healing [44].

Another significant advantage of TCP is its ability to promote angiogenesis. Calcium phosphate-based biomaterials, including TCP, have been reported to enhance neovascularization, which is crucial for delivering oxygen and nutrients to regenerating tissues. Improved vascularization accelerates tissue remodeling and contributes to faster wound closure [44].

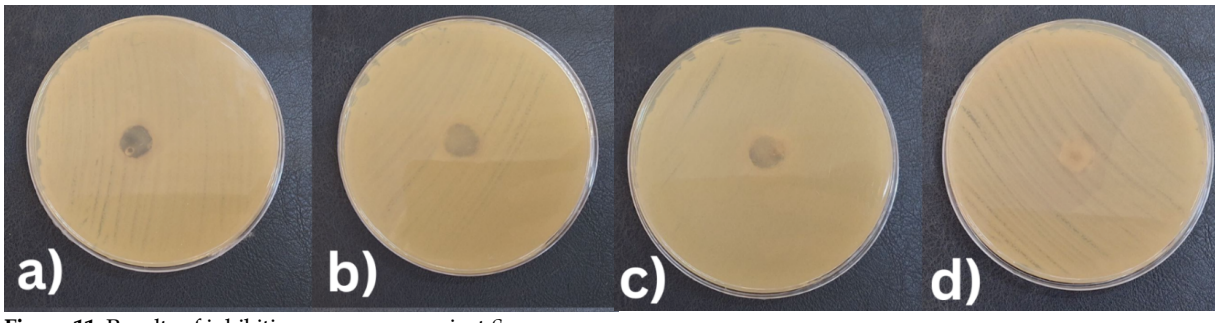


**Figure 11.** Results of inhibition zone assay against *S. aureus*

a) Control sample, b) Scaffold containing 10% β-TCP, c) Scaffold containing 20% β-TCP, d) Scaffold containing 30% β-TCP

Therefore, although TCP does not directly prevent bacterial colonization, its incorporation into wound dressings and tissue-engineered scaffolds can significantly improve the healing process by enhancing cell adhesion, stimulating angiogenesis, supporting extracellular matrix formation, and providing sustained release of biologically active ions. Consequently, TCP is often combined with antibacterial agents such as silver nanoparticles, zinc oxide, antibiotics, or bioactive polymers to simultaneously achieve antimicrobial protection and enhanced tissue regeneration [43, 44].

## Conclusion

In this study, a biodegradable cellulose-based hydrogel scaffold composed of HEC, HPMC, gelatin, and β-TCP was successfully fabricated through freeze-drying and genipin-mediated crosslinking for potential wound-healing applications. Optimization of the polymer composition demonstrated that the HEC70–HPMC30 formulation provided the most favorable mechanical properties, exhibiting a tensile strength of nearly 30 MPa and a Young's modulus of about 1800 MPa while maintaining adequate flexibility. The incorporation of genipin-crosslinked gelatin substantially enhanced scaffold stability by extending the degradation time from approximately 1 to 24 h. Furthermore, β-TCP incorporation significantly modified scaffold morphology, producing a more homogeneous and organized porous structure and improving the distribution of bioactive mineral phases throughout the matrix. Increasing β-TCP concentration reduced water uptake from 712% to 402% and reduced scaffold degradation to approximately 85% after 24 h, indicating enhanced resistance to swelling and hydrolytic degradation. FTIR and elemental mapping analyses confirmed the successful incorporation and homogeneous dispersion of β-TCP within the scaffold network. Although no antibacterial activity was observed against *E. coli* or *S. aureus*, the presence of β-TCP is expected to promote tissue regeneration by its bioactivity, biodegradability, and ability to release calcium and phosphate ions, which support cellular activities associated with wound healing.

Overall, the developed HEC/HPMC/gelatin/β-TCP scaffold combines favorable mechanical performance, controlled degradation, high porosity, and improved structural stability, highlighting its potential as a promising wound dressing and tissue-engineering platform. Future studies should focus on biological evaluations, including cytocompatibility, cell proliferation, and in vivo wound-healing assessments, as well as the incorporation of antibacterial agents to further enhance clinical applicability.

## Ethical Considerations

### Compliance with ethical guidelines

There were no ethical considerations to be considered in this research.

### Funding

This study was financially supported by Materials and Energy Research Center (MERC), Karaj. Iran (Grant No.: 771401058).

### Authors' contributions

Conceptualization: Nader Nezafati and Elham Taghizadeh; Methodology: Nader Nezafati, Maryam Tahmasebi, and Elham Taghizadeh; Writing the original draft: Maryam Tahmasebi; Data interpretation, review and editing: All authors; Resources, supervision and project administration: Nader Nezafati and Saeed Hesaraki.

### Conflict of interest

The authors declared no conflict of interest.

### Acknowledgments

The authors would like to acknowledge the Materials and Energy Research Center (MERC) for its experimental laboratories in performing this research work.

### References

[1] Osanloo M, Noori F, Varaa N, Tavassoli A, Goodarzi A, Moghaddam MT, et al. The wound healing effect of polycaprolactone-chitosan scaffold coated with a gel containing Zataria multiflora Boiss. volatile oil nanoemulsions. BMC Complementary Medicine and Therapies. 2024; 24(1):56. [DOI:10.1186/s12906-024-04352-1] [PMID] [PMCID]

[2] Aadil KR, Nathani A, Rajendran A, Sharma CS, Lenka N, Gupta P. Investigation of human hair keratin-based nanofibrous scaffold for skin tissue engineering application. Drug Delivery and Translational Research. 2024; 14(1):236-46. [DOI:10.1007/s13346-023-01396-7] [PMID]

[3] Naeem A, Yu C, Wang X, Peng M, Liu Y, Liu Y. Hydroxyethyl cellulose-based hydrogels as controlled release carriers for amorphous solid dispersion of bioactive components of radix Paeonia alba. Molecules. 2023; 28(21):7320. [DOI:10.3390/molecules28217320] [PMID] [PMCID]

[4] Ko GR, Lee JS. Engineering of immune microenvironment for enhanced tissue remodeling. Tissue Engineering and Regenerative Medicine. 2022; 19(2):221-36. [DOI:10.1007/s13770-021-00419-z] [PMID] [PMCID]

[5] Yim H, Cho YS, Seo CH, Lee BC, Ko JH, Kim D, et al. The use of AlloDerm on major burn patients: AlloDerm prevents post-burn joint contracture. Burns. 2010; 36(3):322-8. [DOI:10.1016/j.burns.2009.10.018] [PMID]

[6] Stone RC, Stojadinovic O, Rosa AM, Ramirez HA, Badiavas E, Blumenberg M, et al. A bioengineered living cell construct activates an acute wound healing response in venous leg ulcers. Science Translational Medicine. 2017; 9(371):eaaf8611. [DOI:10.1126/scitranslmed.aaf8611] [PMID] [PMCID]

[7] Fan C, Pek CH, Por YC, Lim GJS. Biobrane dressing for paediatric burns in Singapore: A retrospective review. Singapore Medical Journal. 2018; 59(7):360-5. [DOI:10.11622/smedj.2017116] [PMID] [PMCID]

[8] Marston WA, Hanft J, Norwood P, Pollak R; Dermagraft Diabetic Foot Ulcer Study Group. The efficacy and safety of dermagraft in improving the healing of chronic diabetic foot ulcers: Results of a prospective randomized trial. Diabetes Care. 2003; 26(6):1701-5. [DOI:10.2337/diacare.26.6.1701] [PMID]

[9] Driver VR, Lavery LA, Reyzelman AM, Dutra TG, Dove CR, Kotsis SV, et al. A clinical trial of Integra Template for diabetic foot ulcer treatment. Wound Repair and Regeneration. 2015; 23(6):891-900. [DOI:10.1111/wrr.12357] [PMID]

[10] Lukish JR, Eichelberger MR, Newman KD, Pao M, Nobuhara K, Keating M, et al. The use of a bioactive skin substitute decreases length of stay for pediatric burn patients. Journal of Pediatric Surgery. 2001; 36(8):1118-21. [DOI:10.1053/jpsu.2001.25678] [PMID] [PMCID]

[11] Janmohammadi M, Nazemi Z, Salehi AOM, Seyfoori A, John JV, Nourbakhsh MS, et al. Cellulose-based composite scaffolds for bone tissue engineering and localized drug delivery. Bioactive Materials. 2023; 20:137-63. [DOI:10.1016/j.bioactmat.2022.05.018] [PMID] [PMCID]

[12] Sun N, Wang T, Yan X. Self-assembled supermolecular hydrogel based on hydroxyethyl cellulose: Formation, in vitro release and bacteriostasis application. Carbohydrate Polymers. 2017; 172:49-59. [DOI:10.1016/j.carbpol.2017.05.026] [PMID]

[13] Fu LH, Qi C, Ma MG, Wan P. Multifunctional cellulose-based hydrogels for biomedical applications. Journal of Materials Chemistry B. 2019; 7(10):1541-62. [DOI:10.1039/C8TB02331J] [PMID]

[14] Khater ES, Bahnasawy A, Gabal BA, Abbas W, Morsy O. Effect of adding nano-materials on the properties of hydroxypropyl methylcellulose (HPMC) edible films. Scientific Reports. 2023; 13(1):5063. [DOI:10.1038/s41598-023-32218-y] [PMID] [PMCID]

[15] Liu W, Zhang J, Rethore G, Khairoun K, Pilet P, Tancret F, et al. A novel injectable, cohesive and toughened Si-HPMC (silanized-hydroxypropyl methylcellulose) composite calcium phosphate cement for bone substitution. Acta Biomaterialia. 2014; 10(7):3335-45. [DOI:10.1016/j.actbio.2014.03.009] [PMID]

[16] Shao X, Sun H, Zhou R, Zhao B, Shi J, Jiang R, et al. Effect of bovine bone collagen and nano-TiO2 on the properties of hydroxypropyl methylcellulose films. International Journal of Biological Macromolecules. 2020; 158:937-44. [DOI:10.1016/j.ijbiomac.2020.04.107] [PMID]

[17] Shahitha F, Al-Mamari A, Al-Sibani M, Amri IS, Harrasi AA. Environmental-friendly hydrogels from hydroxyethyl cellulose (HEC)/sodium alginate (SA)/hyaluronic acid (HA) for wound healing applications. International Journal of Latest Technology in Engineering, Management & Applied Science. 2025; 14(9):684-94. [Link]

[18] Zulkifli FH, Hussain FS, Rasad MS, Yusoff MM. In vitro degradation study of novel HEC/PVA/collagen nanofibrous scaffold for skin tissue engineering applications. Polymer Degradation and Stability. 2014; 110:473-81. [DOI:10.1016/j.polymdegradstab.2014.10.017]

[19] Tudoroiu EE, Dinu-Pîrvu CE, Albu Kaya MG, Popa L, Anu□a V, Prisada RM, et al. An Overview of Cellulose Derivatives-Based Dressings for Wound-Healing Management. Pharmaceuticals (Basel). 2021; 14(12):1215. [DOI:10.3390/ph14121215] [PMID] [PMCID]

[20] Wang X, Tang M. Bioceramic materials with ion-mediated multifunctionality for wound healing. Smart Medicine. 2022; 1(1):e20220032. [DOI:10.1002/SMMD.20220032] [PMID] [PMCID]

[21] Haghighizadeh E, Shahrezaee M, Sharifzadeh SR, Momeni M. Transforming growth factor-β3 relation with osteoporosis and osteoporotic fractures. Journal of Research in Medical Sciences. 2019; 24:46. [DOI:10.4103/jrms.JRMS_1062_18] [PMID] [PMCID]

[22] Gao C, Deng Y, Feng P, Mao Z, Li P, Yang B, et al. Current progress in bioactive ceramic scaffolds for bone repair and regeneration. International Journal of Molecular Sciences. 2014; 15(3):4714-32. [DOI:10.3390/ijms15034714] [PMID] [PMCID]

[23] Subramaniam T, Fauzi MB, Lokanathan Y, Law JX. The role of calcium in wound healing. International Journal of Molecular Sciences. 2021; 22(12):6486. [DOI:10.3390/ijms22126486] [PMID] [PMCID]

[24] Rossi F, Perale G, Masi M. Biological buffered saline solution as solvent in agar-carbomer hydrogel synthesis. Chemical Papers. 2010; 64(5):573-8. [DOI:10.2478/s11696-010-0052-4]

[25] Derakhshani A, Hesaraki S, Nezafati N, Azami M. Wound closure, angiogenesis and antibacterial behaviors of tetracalcium phosphate/hydroxyethyl cellulose/hyaluronic acid/gelatin composite dermal scaffolds. Journal of Biomaterials Science. Polymer Edition. 2022; 33(5):605-26. [DOI:10.1080/09205063.2021.2008786] [PMID]

[26] O'Brien FJ, Harley BA, Yannas IV, Gibson LJ. The effect of pore size on cell adhesion in collagen-GAG scaffolds. Biomaterials. 2005; 26(4):433-41. [DOI:10.1016/j.biomaterials.2004.02.052] [PMID]

[27] Loh QL, Choong C. Three-dimensional scaffolds for tissue engineering applications: Role of porosity and pore size. Tissue engineering. Part B, Reviews. 2013; 19(6):485-502. [DOI:10.1089/ten.teb.2012.0437] [PMID] [PMCID]

[28] Wu X, Liu Y, Li X, Wen P, Zhang Y, Long Y, et al. Preparation of aligned porous gelatin scaffolds by unidirectional freeze-drying method. Acta Biomaterialia. 2010; 6(3):1167-77. [DOI:10.1016/j.actbio.2009.08.041] [PMID]

[29] Rezwan K, Chen QZ, Blaker JJ, Boccaccini AR. Biodegradable and bioactive porous polymer/inorganic composite scaffolds for bone tissue engineering. Biomaterials. 2006; 27(18):3413-31. [DOI:10.1016/j.biomaterials.2006.01.039] [PMID] [PMCID]

[30] Boccaccini AR, Maquet V. Bioresorbable and Bioactive Polymer/Bioglass Composites with Tailored Pore Structure for Tissue Engineering Applications. Composites Science and Technology. 2003; 63(16):2417-29. [Link]

[31] Haugh MG, Murphy CM, O'Brien FJ. Novel freeze-drying methods to produce a range of collagen-glycosaminoglycan scaffolds with tailored mean pore sizes. Tissue Engineering. Part C, Methods. 2010; 16(5):887-94. [DOI:10.1089/ten.tec.2009.0422] [PMID]

[32] Balgude D, Konge K, Sabnis A. Synthesis and characterization of sol-gel derived CNSL based hybrid anti-corrosive coatings. Journal of Sol-Gel Science and Technology. 2014; 69(1):155-65. [DOI:10.1007/s10971-013-3198-z]

[33] Kucharska M, Butruk B, Walenko K, Brynk T, Ciach T. Fabrication of in-situ foamed chitosan/β-TCP scaffolds for bone tissue engineering application. Materials Letters. 2012; 85:124-7. [Link]

[34] Peter M, Ganesh N, Selvamurugan N, Nair SV, Furuike T, Tamura H, et al. Preparation and characterization of chitosan–gelatin/nanohydroxyapatite composite scaffolds for tissue engineering applications. Carbohydrate Polymers. 2010; 80(3):687-94. [Link]

[35] Bohner M, Santoni BLG, Döbelin N. β-tricalcium phosphate for bone substitution: Synthesis and properties. Acta Biomaterialia. 2020; 113:23-41. [DOI:10.1016/j.actbio.2020.06.022] [PMID]

[36] Yavari L, Ghorbani M. A novel aloe vera-loaded ethylcellulose/hydroxypropyl methylcellulose nanofibrous mat designed for wound healing application. 2021. [Preprint]. [DOI:10.21203/rs.3.rs-517639/v1]

[37] Maji K, Dasgupta S. Effect of βtricalcium phosphate nanoparticles additions on the properties of gelatin-chitosan scaffolds. Bioceramics Development and Applications. 2017; 7:2. [DOI:10.4172/2090-5025.1000103]

[38] Ortega-Toro R, Jiménez A, Talens P, Chiralt A. Properties of starch-hydroxypropyl methylcellulose based films obtained by compression molding. Carbohydrate Polymers. 2014; 109:155-65. [DOI:10.1016/j.carbpol.2014.03.059] [PMID]

[39] Demitri C, Del Sole R, Scalera F, Sannino A, Vasapollo G, Maffezzoli A, et al. Novel superabsorbent cellulose-based hydrogels crosslinked with citric acid. Journal of Applied Polymer Science. 2008; 110(4):2453-60. [DOI:10.1002/app.28660]

[40] Hashimoto K, Oikawa H, Shibata H. Characterization of porous β-type tricalcium phosphate ceramics formed via physical foaming with freeze-drying. International Journal of Molecular Sciences. 2024; 25(10):5363. [DOI:10.3390/ijms25105363] [PMID] [PMCID]

[41] Umrath F, Schmitt LF, Kliesch SM, Schille C, Geis-Gerstorfer J, Gurewitsch E, et al. Mechanical and functional improvement of β-tcp scaffolds for use in bone tissue engineering. Journal of Functional Biomaterials. 2023; 14(8):427. [DOI:10.3390/jfb14080427] [PMID] [PMCID]

[42] Spirandeli BR, Martins EF, Dona LR, Ribas RG, Campos TM, Esposito E, et al. Synergistic effect of incorporation of BG 45S5 and silver nanoparticles on β-TCP scaffolds: Structural characterization and evaluation of antimicrobial activity and biocompatibility. Materials Research. 2023; 26:e20230137. [DOI:10.1590/1980-5373-mr-2023-0137]

[43] Lu J, Yu H, Chen C. Biological properties of calcium phosphate biomaterials for bone repair: A review. RSC Advances. 2018; 8(4):2015-33. [DOI:10.1039/C7RA11278E] [PMID] [PMCID]

[44] Lu H, Zhou Y, Ma Y, Xiao L, Ji W, Zhang Y, et al. Current application of beta-tricalcium phosphate in bone repair and its mechanism to regulate osteogenesis. Frontiers in Materials. 2021; 8:698915. [DOI:10.3389/fmats.2021.698915]